استخلاص الثوابت البصرية و معاملات التشتت للأغشية الرقيقة ثنائية الطبقة CdTe/CdSe

Extraction of Optical Constants and Dispersion Parameters of CdTe/CdSe Bi–Layer Thin Films

د. عبدالناصر عبدالرحمن محمد الفقير[1]

Dr.Abdulnasser Abdulrahman Alfaqeer

د. أحمد محمد الرباطي[2]

Dr.Ahmed Mohammed Abdo Alrebati

– د. مهدي احمد دبان[3]

Dr.Mehdi Ahmed Mohamed Dabban

https://doi.org/10.54582/TSJ.2.2.52

(1) أستاذ الفيزياء المساعد، بكلية التربية والعلوم، جامعة إقليم سبأ/مأرب/ اليمن

عنوان المراسلة : nasser_alfageer@yahoo.com

(2) أستاذ الفيزياء المساعد، بكلية التربية والعلوم، جامعة إقليم سبأ/مأرب/ اليمن

عنوان المراسلة : alribaty@hotmail.com

(3) أستاذ الفيزياء المساعد ،كلية العلوم،جامعة عدن

عنوان المراسلة : mehdi.ahmed.scie@aden-univ.net

المُلخّص :

ركزت الدراسة الحالية على دراسة آثر التلدين الحراري على الثوابت البصرية ومعاملات التشتت للأغشية الرقيقة CdTe /CdSe ثنائية الطبقة المرسبة على ركائز زجاجية بتقنية التبخير الحراري. بيَّن الانزياح الطفيف في عتبة النفاذية نحو منطقة الطول الموجي الأعلى مع زيادة درجة حرارة التلدين الانخفاض المنتظم في فجوة نطاق الطاقة الضوئية (1.92 إلى 1.37 فولت) للأغشية الرقيقة المدروسة. كما أظهر منحنى التشتت لمعامل الانكسار تشتتًا شاذًا في منطقة الامتصاص وتشتتًا طبيعيًا في المنطقة الشفافة. لوحظ أن بيانات التشتت تمتثل لنموذج المتذبذب الفردي Wemple-Didomenico single-oscillator model ، والذي من خلاله تم تحديد معاملات التشتت وثوابت العزل الكهربائية. أدت الزيادة في معامل الانكسار مع درجة حرارة التلدين إلى تعديل المتغيرات الخطية الأخرى مثل الموصلية البصرية ، وعامل التبديد ، والحجم ، فقدان الطاقة السطحية. كما أكدت الزيادة في قيمة الموصلية الضوئية إمكانية استخدام غشاء CdSe كطبقة ماصة للخلايا الشمسية شبه الشفافة. لقد حاولنا مناقشة هذه النتائج وربطها بدرجة حرارة التلدين والآليات المحتملة الكامنة وراء تلك التغيرات..

الكلمات المفتاحية: الأغشية الرقيقة CdTe/CdSe- الثوابت بصرية – معاملات التشتت- الموصلية البصرية

Abstract

The current study focuses on the annealing-induced changes in the optical constants and dispersion parameters of the CdTe/CdSe bi-layer films deposited onto glass substrates by thermal evaporation technique. The slight shift in transmission threshold towards higher wavelength region with increasing annealing temperature revealed the systematic reduction in optical energy band gap (1.92 to 1.37 eV) of the films. The dispersion curve of the refractive index shows an anomalous dispersion in the absorption region and a normal dispersion in the transparent region. It was observed that the dispersion data obeyed the single oscillator of the Wemple-Didomenico model, from which the dispersion parameters and dielectric constants were evaluated. The increase in the refractive index with the annealing temperature modified the other linear parameters such as optical density, dissipation factor, volume, and surface energy loss function. The increase in the optical conductivity value is good for the CdSe film to be used as a semitransparent solar cells absorbing layer. We have made an attempt to discuss and correlate these results with the annealing temperature of possible mechanisms underlying the phenomena.

Keywords: CdTe/CdSe thin films- optical constants- dispersion parameters- optical conductivity.

1. Introduction

Cadmium Selenide (CdSe) is an n-type, reddish semiconductor material. CdSe thin films have been used in photovoltaic devices because of their suitable direct band gap (about 1.74 eV for bulk CdSe material), high absorption coefficient and electrical conductivity [1,2]. Cadmium telluride (CdTe) is II-VI crystalline compound with a zinc blende crystal structure and has a direct bandgap of 1.44 eV [3] which is suitable for electronic applications such as photovoltaic devices [4] light-emitting diodes [5,6] solar cells [7,8] X-ray and gamma detectors [9] Field Effect Transistors (FETS) [10] Lasers [11] and non-linear integrated optical devices [12].The optical dispersion plays an important role in the research for optical materials because it is a significant factor in optical communication and in designing optical devices such as switches, filters, and modulators, etc., where the refractive index of material is the key parameter for device design [13]. CdTe thin films are used as an absorber layer in semitransparent

https://doi.org/10.54582/TSJ.2.2.52

thin film solar cells [14], but there is no report about the usage of CdSe thin films as an absorber layer in semitransparent solar cells.

To the researchers' best knowledge, less attention has been paid to the optical constant and dispersion parameters of the CdTe/CdSe Bi-layer films and consequently less research has been done in this area, hence the obtained findings may be useful for the basic knowledge on this composition for new researcher working in the field of chalcogenide glasses. In our recent articles [15], we studied the effect of annealing and microstructure and optical properties of CdTe/CdSe heterojunction thin films. These investigations revealed that the annealing process leads to the decrease in the values of the optical band gap (E_g), microstrain and dislocation density, while thermal annealing induces an increases of the crystalline size and the values of the width of localized states (E_e). In the present work, these investigations are extended by studying dispersive optical constants changes due to annealing temperature for the thermally deposited CdTe/CdSe bi-layer films in the UV–Vis-NIR wavelength region. Besides, it is concerned essentially with an ability the CdSe film to be used as a semitransparent solar cells absorbing layer with analysis of the dispersive optical constants by focusing on the optical dispersion parameters of these films.

2. ***Experimental details***

The CdTe and CdSe glasses were prepared from high-purity elements by the conventional melt-quench technique. Cd, Se, and Te

https://doi.org/10.54582/TSJ.2.2.52

(Aldrich Chem. Co, USA) weighted according to their atomic percentage by an automatic electrical sensitive balance of accuracy 0.0001 gm and were sealed in pre-cleaned silica-glass ampoules under a vacuum of 10^{-5} Torr. The sealed ampoules were heated up gradually to 1100 K and kept at that temperature for 24 hours. Continuous stirring of the melt was carried out to ensure good homogeneity. The melt was then rapidly quenched in ice water. After quenching, the solid ingots were removed from the ampoules and kept in a dry atmosphere. To prepare the CdTe/CdSe bi-layer thin film, CdTe is deposited on a predeposited CdSe film of thickness 200 nm, up to a thickness of 160 nm by thermal evaporation technique on cleaned glass substrates at room temperature (300 K) using a high-vacuum coating unit (Edwards E 306 A). The working vacuum was kept at about $\sim 10^{-5}$ Torr during deposition. The rate of the film deposition was approximately 6 nm/sec. The film thickness was determined using quartz crystal thickness monitor (FTMS). The thermal annealing of the samples was carried out in an electrical furnace under nitrogen flow at (323, 373،423 and 473 K) for 30 min.

The optical transmittance $T(\lambda)$ and reflectance $R(\lambda)$ of the as-deposited and annealed CdTe/CdSe thin films were measured at room temperature (~ 30 °C) and atmospheric pressure with unpolarized light at normal incidence in the wavelength range of 200–2500 nm using LAMBDA 750 UV/VIS/NIR computer-controlled spectrophotometer attached to a personal computer. A specular reflection stage was

https://doi.org/10.54582/TSJ.2.2.52

attached to measure the reflectivity at normal incidence using an Al mirror as a standard reference. The effect of the substrate on the optical parameters was excluded by utilizing a glass substrate as reference during the optical measurements.

3. Results and discussion

3.1 Optical measurements, T (λ) and R (λ)

In this work, the linear optical parameters of the as-prepped and annealed CdTe/CdSe bi-layer thin films were computed by determining the transmittance T(λ) and reflectance and R(λ) data. The spectral distribution of T(λ) and R(λ) at normal incidence in the wavelength 200-2500 nm for as-prepped and annealed CdTe/CdSe thin films on a glass substrate are presented in **Fig. 1(a-b)**.The general features of this spectrum are as follows:

i. The transmission of the investigated films increases up to a maximum in the range 1290–1370 nm, and then decreases with the further increase of the wavelength. The sharp absorption edges of the as-prepared CdTe/CdSe thin films are in the visible spectral range. Hence, it can be revealed that the optical energy gaps of the as-prepared thin films are in the range of the energy of the visible region. Also, the position of the fundamental absorption edge shifts to lower energy with increasing annealing temperature (*i.e.*, the blue shift of the optical absorption edge), as previously mentioned [15]. The presence of such a sharp absorption edge in T(λ) spectra recommends CdTe/CdSe thin films as a good optical filter material.

ii. Some oscillations curve could be seen in the R(λ) at various λ as a result of the interference phenomena. Generally, oscillations observed in the R(λ) spectra reveal the optical homogeneity of the prepared samples.

iii. It is worth mentioning that T and R spectra analysis for as-prepared CdTe/CdSe bi-layer thin films displays that at short wavelengths that the sum of their intensities is less than the unity ($T+R \ll 1$); but with increases the wavelength, it is almost approaches to the unity, where $T+R \approx 1$. This indicates that at higher wavelengths in the NIR-region the absorption nature of as- prepared CdTe/CdSe thin films becomes very small.

iv. Finally, the intensity of T-spectra decreases, whilst that of R-spectra increases with the increasing the annealing of CdTe/CdSe bi-layer thin films along all the studied spectra, but the sum of intensities T and R spectra at the near-infrared region is less than for as-prepared indicating that the annealed CdTe/CdSe thin films become obscure. This almost owes the increased absorption of the samples, as it will be observed in our previous study [15].The important feature of such changes in T(λ) with annealing is to control the spectral range of photosensitivity of the CdTe/CdSe bi-layer thin films.

https://doi.org/10.54582/TSJ.2.2.52

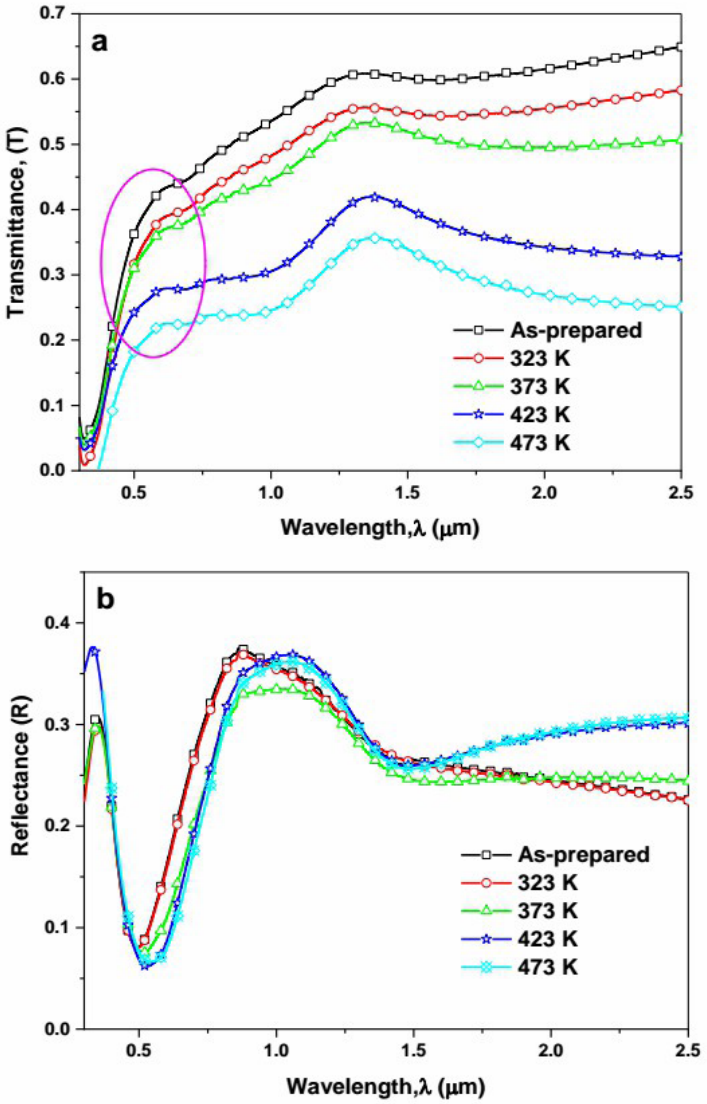

Fig.1: Spectral behavior of (a) T(λ) and (b) R(λ) for CdTe/CdSe bi-layer thin films.

https://doi.org/10.54582/TSJ.2.2.52

3.2 Optical constants and dispersion analysis

The complex refractive index, $\tilde{n} = n + ik_{ex}$ characterizes the optical properties of many solid materials. To obtain the optical constants (the refractive index n and absorption index k for the investigated films, Murmann's exact equations [16,17] have been applied in conjunction with a special iterative computer program (Eureka, the solver). It is based on minimizing $(\Delta R)^2$ and $(\Delta R)^2$ simultaneously, where:

$$(\Delta R)^2 = \left|R_{cal}(n,k,d,\lambda) - R_{\exp}\right|^2$$
$$(\Delta T)^2 = \left|T_{cal}(n,k,d,\lambda) - T_{\exp}\right|^2 \quad (1)$$

where $R_{\exp}$ and $T_{\exp}$ are the experimentally determined values of T and R, respectively, and R_{cal} and T_{cal} are the calculated values of T and R, using Murmann's equation. The adapted computation steps are as follows:

1. The measured transmittance, $T_{\exp}$, measured reflectance $R_{\exp}$, film thickness; d and the refractive index of substrate n_s are entered.
2. The film thickness d is an important parameter in the accurate determination of the optical constant. Therefore, different methods have been used for determination of the thickness of the deposited films. Such thickness has been firstly estimated in situ by using a quartz crystal thickness monitor.

https://doi.org/10.54582/TSJ.2.2.52

3. This method requires approximate values of n and k. The approximate values n and k were obtained using the following equations [18]:

$$n = \frac{1+R_{exp}}{1-R_{exp}} + \left[\left(\frac{R_{exp}+1}{R_{exp}-1}\right)^2 - (1+k^2)\right]^{1/2} \quad (2)$$

$$\alpha = \frac{1}{d}\ln\left[\frac{(1-R_{exp})^2}{2T_{exp}} + \left\{\left(\frac{(1-R_{exp})^2}{2T_{exp}}\right)^2 - R_{exp}{}^2\right\}^{\frac{1}{2}}\right] \quad (3)$$

$$k = \frac{\alpha\lambda}{4\pi} \quad (4)$$

4. Using the experimental values of T(λ) and R(λ), it is easy to solve Murmann's exact equations for transmittance and reflectance simultaneously to obtain the accurate values of n and k using the iterative technique through initial approximations for n and k.
5. Using the Murmann's equation, both R_{cal} and T_{cal} are calculated throughout the whole ranges.
6. In each step the variances $(\Delta R)^2$ and $(\Delta T)^2$ are calculated and compared, to seek their simultaneous minimization. The corresponding values of n and k represent the solution. During the iteration, in some small regions of the spectrum the solutions may be missing. The missing part can be interpolated by using the program origin version 2019 (OriginLab Corp.).

https://doi.org/10.54582/TSJ.2.2.52

The spectral distributions of values of both $k(\lambda)$ and $n(\lambda)$ for the as-prepared and annealed CdTe/CdSe bi-layer thin films on the wavelength of the incident light are shown in **Fig. 2 (a-b)** respectively. Based on **Fig. 2(a)**, the value of k for the as-prepared and annealed CdTe/CdSe bi-layer thin films decreased with an increase in a whole range of the wavelength. In addition, the estimated value of k increased with an increase in annealing temperature. The increase in k may be attributed to the increase in the average crystallites size with increasing annealing temperature of the studied films. Furthermore, It could be observed that the refractive index, n (**Fig 2. b**) shows anomalous dispersion in the low wavelength range ($400 \leq \lambda \leq 1100$ nm) (Absrption region), while for long wavelength ($\lambda > 1100$ nm), decreases monotonically (transparent region), which fact may be attributed to the effect of free carrier concentration. The reduction inn values at $\lambda > 1100$ nm revealed the normal dispersion trends of the chalcogenide semiconductors [19].It is worth mentioning that the n values had a maximum value at $\lambda = 850–1100$ nm for the as-prepared and annealed CdTe/CdSe bi-layer thin films. The maximum value of refractive index suffered a shift towards the longer wavelength as the annealing temperatures this behavior can be attributed to increase tailing [20].

https://doi.org/10.54582/TSJ.2.2.52

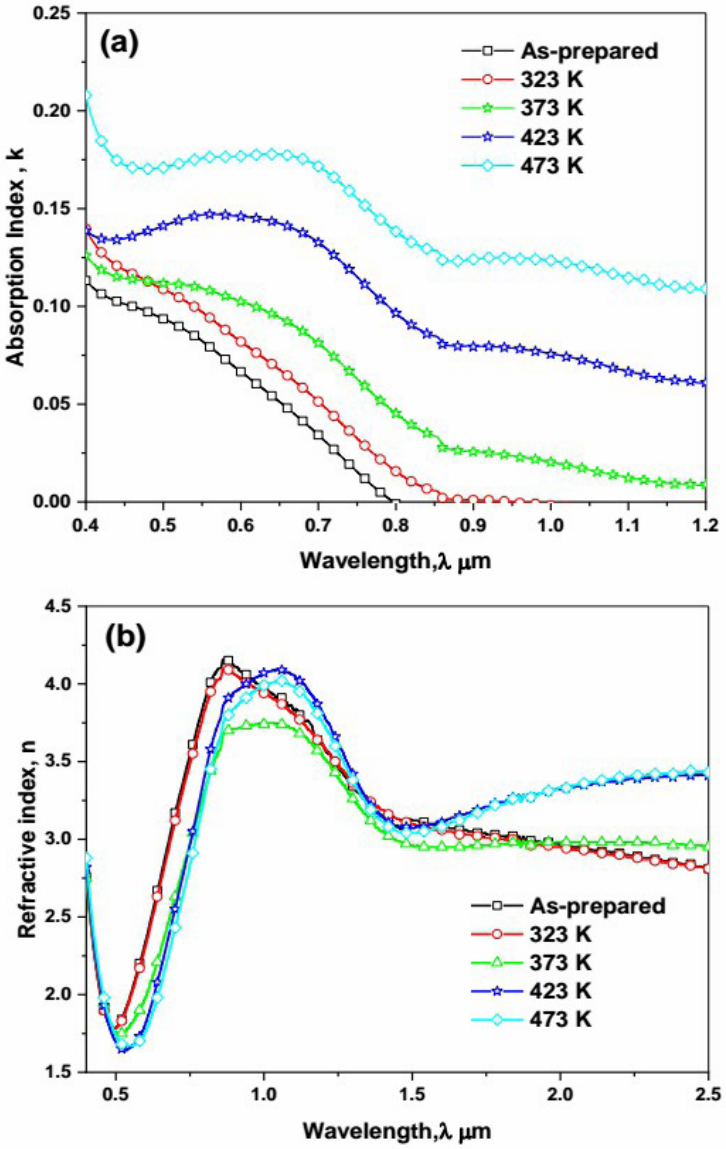

Fig. 2: Spectral distribution of: (a) absorption index (k) and (b) refractive index (n) for CdTe/CdSe bi-layer thin films

https://doi.org/10.54582/TSJ.2.2.52

The Wemple and DiDomenico (WDD) single oscillator model was performed to investigate the dispersion behavior of n through the following relation [21,22]:

$$n^2 = 1 + \frac{E_d E_o}{E_o^{\,2} - (h\nu)^2} \tag{5}$$

where E_o is the oscillator energy and considered as an average energy gap (The physical meaning of E_o is that it stimulates all the electronic excitation involved and take values near the main peak of the imaginary part of the dielectric constant spectrum), and E_d is the dispersion energy which measures the average strength of the interband optical transitions and is related to the chemical bonding and the charge distribution within each unit cell. In addition, determination of the dispersion energy plays a major role in determining the behavior of the refractive indices and properly normalizes the interaction potential describing these optical effects which is due to the relationship between the electronic and optical properties of the material and its chemical bonds. In particular, Wemple-DiDomenico showed that E_d does not depend on either the band gap or the volume density of the valence electrons, but it depends on the chemical bonding character of material, coordination number of the cation nearest- neighbor to the anion, formal chemical valance of the anion and the effective number of valence electrons per anion

The dispersion parameters of the investigated films were evaluated to get more understanding of their optical properties. **Fig.3** illustrates

https://doi.org/10.54582/TSJ.2.2.52

the plot of $(n^2-1)^{-1}$ versus $(h\upsilon)^2$for the investigated films, which yields a straight line for normal behavior having the slope $(E_oE_d)^{-1}$ and the intercept with the vertical axis is E_o/E_d from which E_o and E_d can be directly determined from **Eq. 5**. The estimated values of E_o and $E_d$of our samples are listed in **Table 1** and plotted in **Fig. 4**. It is observed that the values of E_o decrease, while E_d increases with increasing the annealing temperature. The increase of E_d with the annealing temperature could be attributed to increasing the rate of atomic diffusion in the annealed thin films, indicating an increase in the number of atoms at interstitial sites which causes a formation of the impurity type scattering centers. The reduction in oscillator energy is associated with the decrease in energy band gap (Tauc energy), i.e. the greater the lattice oscillator energy, the greater the optical band gap[23]. This is not surprising, as the energy of the oscillators is usually believed to be the overall energy of the material. It is evident from **Table1**that the average ratio of $E_o/E_g \approx 2$, which is in good agreement with that mentioned by Tanaka [24]. The dependence of E_o and E_d on the annealing temperature T_A can be fitted to a polynomial function of the form:

$$E_o = 159.03508 - 1.70076\,T_A + 0.00694\,T_A^2 - 1.24782\times10^{-5}T_A^3 + 8.33442\times10^{-9}T_A^4 \ (eV) \quad (6)$$

$$E_d = 0.50496 + 0.03136\,T_A \ (eV) \quad (7)$$

On the other hand, the static refractive index (n_0) of the investigated thin films was evaluated by extrapolated the *WDD*

https://doi.org/10.54582/TSJ.2.2.52

dispersion relation, **Eq. 5**, using conditions when $n = n_0$ will $h\nu \to 0$ and this suggestion gives:

$$n_0 = \sqrt{1 + \frac{E_d}{E_o}} \tag{8}$$

The numerical values of $n_0$for the studied thin films are listed in **Table 1**.The static dielectric constant ε_∞ was calculated for the as-prepared and annealed CdTe/CdSe bi-layer thin films using $\varepsilon_\infty = n_0^2$ and tabulated in **Table 1**. The evaluated values of $n_0$and ε_∞ increased with an increase in annealing temperature T_A. Besides, E_g and ε_∞seemed to change in the opposite manner which is in agreement with the relation, $\varepsilon_\infty^2 \times E_g = const.$, suggested by Moss et al. [25].The oscillator strength is one the important parameters obtained from the WDD model and is calculated by taking the product of E_0 and E_d, i.e.$f = E_0E_d$. The obtained 'f' value is given in **Table 1**, and it is seen that its value increased for the CdTe/CdSe bi-layer thin films with annealing. On the other hand, a measure of inter-band transition strengths can be provided from the first-order (M_{-1}) and third-order optical moments (M_{-3}) of the optical spectrum. The M_{-1} and M_{-3} moments can be computed as [26]:

$$M_{-1} = \frac{E_d}{E_o} \quad , \quad M_{-3} = \frac{E_d}{E_o^3} \tag{9}$$

The evaluated values of M_{-1}vary from 2.75to 5.14 (dimensionless) and

https://doi.org/10.54582/TSJ.2.2.52

M_{-3}lies between 0.21 and 0.58 $(eV)^{-2}$ (**Table1**). Similar results of the moment value range for the other semiconductor films have also been reported [27], which is consistent with our findings. In addition, the dispersion energy E_d is known to follow the empirical relationship [28]:

$$E_d\,(\mathrm{eV}) = \beta\langle r\rangle Z_a N_e \qquad (10)$$

where β is a constant depends on the chemical bonding character of material (0.37 ± 0.04 in covalent materials, and 0.26 ± 0.03 in the more ionic materials), $\langle r\rangle$ is the coordination number of the nearest-neighbour cation, Z_a the formal anion valence and N_e the effective number of valence electrons per anion. Furthermore, it has been reported that the band gap of the material is related to its refractive index approximately by $(n_\infty^2 - 1 = \langle r\rangle Z_a N_e / 6E_g)$ [29]. Thus,

$$\beta = \frac{E_d}{6E_g\,(n_\infty^2 - 1)} \qquad (11)$$

In the present work, calculated β values are in the range of (0.313–0.362) which means that, the bonds in the investigated films have covalent character.

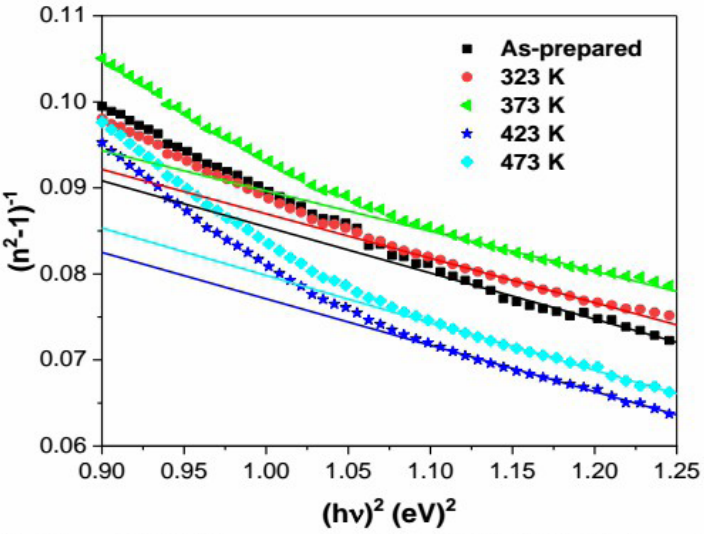

Fig. 3: Plots of $(n^2-1)^{-1}$ versus $(h\nu)^2$ for CdTe/CdSe bi-layer thin films.

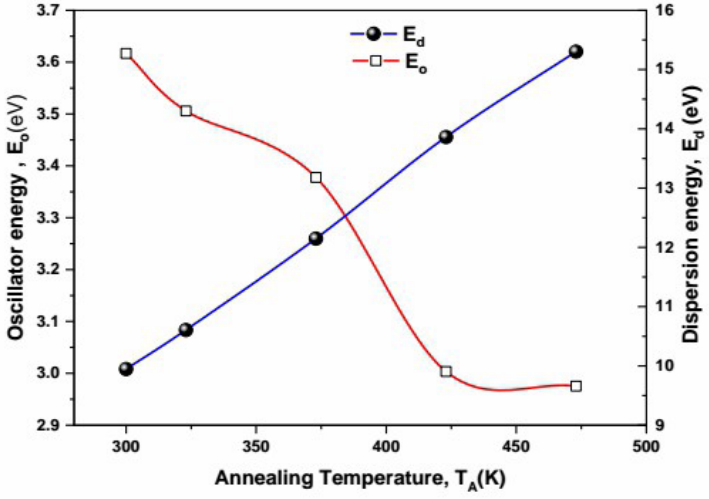

Fig. 4. The values of E_o and E_d as a function of annealing temperature for CdTe/CdSe bi-layer thin films.

https://doi.org/10.54582/TSJ.2.2.52

Table 1: Dispersion and Dielectric parameters of CdTe/CdSe bi-layer thin films.

Dispersion and Dielectric parameters	Annealing Temperatures T_A				
	As	323	373	423	473
Optical band gap E_g (eV)	1.92	1.86	1.63	1.48	1.37
Oscillator energy E_o (eV)	3.62	3.51	3.38	3.00	2.98
Dispersion energy E_d (eV)	9.92	10.60	12.14	13.86	15.30
The ratio of E_o/E_g	1.88	1.89	2.07	2.02	2.17
Static refractive index n_0	1.94	2.01	2.14	2.37	2.48
Static linear dielectric constant ε_∞	3.75	4.02	4.60	5.62	6.14
Oscillator strength f	35.98	37.20	41.03	41.58	45.59
First moments of optical spectra M_{-1}	2.75	3.023	3.56	4.62	5.14
Third-order moments of optical spectra M_{-3} $(eV)^{-2}$	0.21	0.25	0.32	0.51	0.58
Chemical bonding character β	0.313	0.314	0.345	0.338	0.362
Average oscillator wavelength ($\lambda_0 nm$)	685.7	709.0	734.6	827.2	838.3
Average oscillator strength $S_0(\times 10^{13} m^{-2})$	1.17	1.20	1.34	1.35	1.46
The ratio of $E_o/S(\times 10^{-14})$	15.5	14.5	12.7	11.1	10.1
Lattice dielectric constant ε_L	21.64	22.12	22.53	29.83	28.12
Carrier concentration N/m* $(\times 10^{58} m^{-3} kg^{-1})$	4.75	4.92	5.39	8.23	7.57
Plasma frequency ω_P $(\times 10^{15} Hz)$	2.518	2.535	2.630	2.823	2.790

https://doi.org/10.54582/TSJ.2.2.52

The average inter-band oscillator wavelength (λ_o) was estimated based on the classical dispersion relation or the single term Sellmeier oscillation as follows [30,31]:

$$(n^2-1)^{-1} = \frac{1}{S_o \lambda_o^{\,2}} - \frac{1}{S_o}\lambda^{-2} \qquad (12)$$

where S_o is the average oscillator strength ($S_o = (n_\infty^2 - 1)/\lambda_o^2$). Plots of $(n^2\text{-}1)^{-1}$ versus λ^{-2} for as-papered and annealed CdTe/CdSe thin films, which are shown in **Fig. 5**, gives the values of fitting parameters S_o, and λ_o as listed in **Table1**. On the other hand, the ratio of E_o/S_o is of the same order as that obtained by Wemple and Didomenico for some materials belonging to several crystal structures (10^{-14} eV.m^2) [32].

https://doi.org/10.54582/TSJ.2.2.52

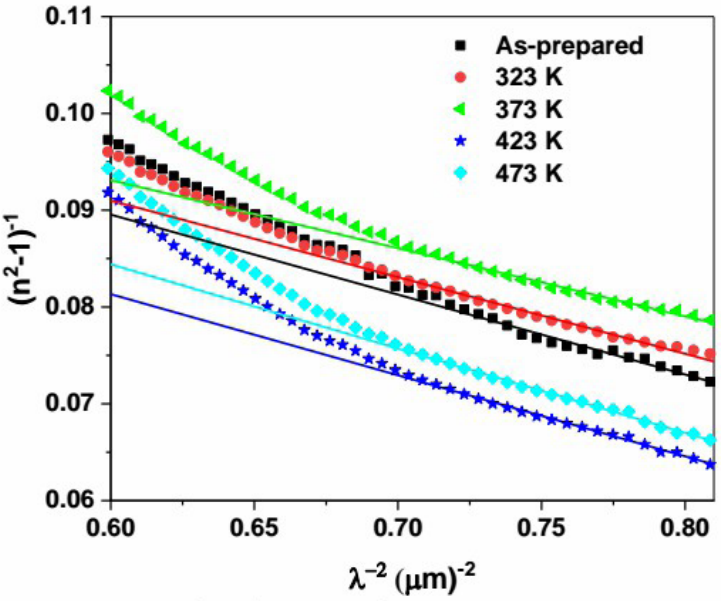

Fig. 5: Plots of $(n^2-1)^{-1}$ versus $\lambda^{-2}$for CdTe/CdSe bi-layer thin films.

The lattice dielectric constant (ε_L) of the investigated samples is calculated using the procedure which takes into consideration the contribution of free carriers and the lattice vibration modes of dispersion using Drude's theory as follows [33]:

$$n^2 = \varepsilon_L - \left(\frac{e^2 N}{4\pi^2 c^2 \varepsilon_o m^*} \right) \lambda^2 \qquad (13)$$

where e is the electronic charge, c is the light velocity, ε_o is the free space dielectric constant (8.845×10^{-12} F/m), N and m^* are the free carrier concentration and its effective mass respectively. **Fig.11** illustrates the plots of n^2 versus λ^2 for the as-prepared and annealed

https://doi.org/10.54582/TSJ.2.2.52

CdTe/CdSe bi-layer thin films and found to be straight lines for verifying **Eq. 13**.

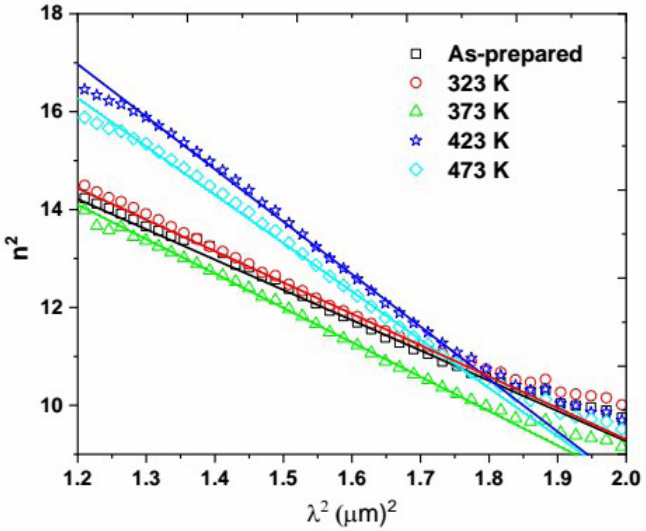

Fig. 6: Plots of n^2 versus λ^2 for CdTe/CdSe bi-layer thin films

From the slope and intercepts of the fitted lines in **Fig. 6**, the values of ε_L and N/m* were deduced for each annealing temperature and listed in **Table1**. The plasma resonance frequency, ω_p (a resonant frequency of free oscillations of the electrons about their equilibrium positions) for one kind of free carriers and can be expressed as:

$$\omega_p = (e^2 N / \varepsilon_o . \varepsilon_{\infty(1)} . m^*)^{1/2} \qquad (14)$$

Using our results of N/m^* and ε_L, the plasma resonance frequency ω_p for one kind of free carrier can be calculated and listed in **Table1**. **Fig.**

7 shows the variation of the ratio N/m^* and ε_L with increasing of T_A. On the one hand, it is clear that both N/m^* and ε_L change in the same manner, Both of ε_L and N/m* enhanced with the increase in T_A which can be attributed to a change in the carrier concentration N when taking into consideration that the effective mass m^* is constant. It is noticed that the values ε_L are higher than those of ε_∞ for all investigated thin films, as a result, to the increase in N [34]. Further, the behavior of plasma frequency ω_p can be reflected by the corresponding change in $\left[(N/m^*)/\varepsilon_{\infty(1)}\right]^{1/2}$. According to Penn's theory [35], which applies to chalcogenide semiconductors, we have:

$n^2 = 1 + \left(\frac{h\omega_p}{E_g}\right)$ (15). Therefore, according to **Eq. 15**, the increase of refractive index with increasing annealing temperature may be due to the increase of the concentration N and hence, to the decrease in the optical energy gap E_g.

https://doi.org/10.54582/TSJ.2.2.52

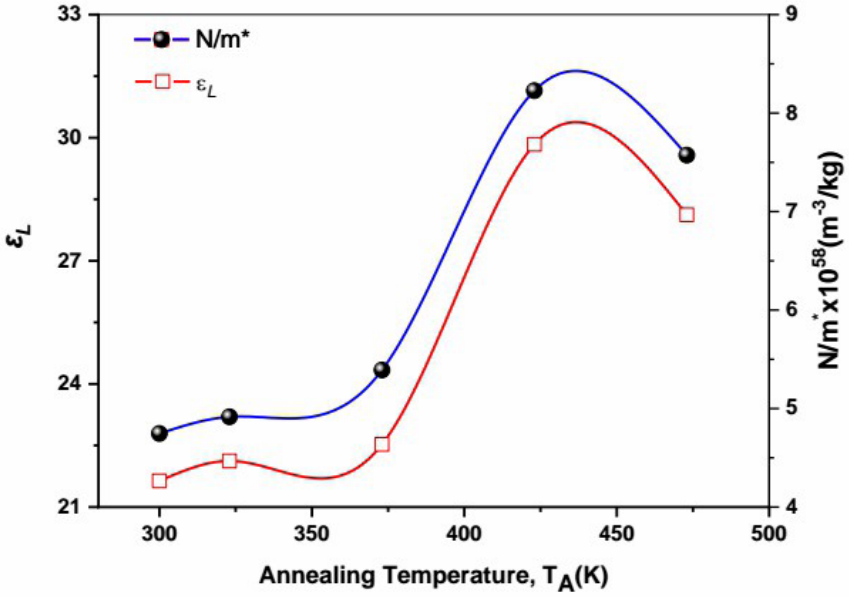

Fig. 7: The variation of the ratio *N/m** and ε_L as function of annealing temperature for CdTe/CdSe bi-layer thin films.

3.3 Dielectric constant parts and dissipation factor

The complex dielectric constant $\tilde{\varepsilon} = \varepsilon_r - i\varepsilon_i$ are to be investigated to understand the optical properties of solid semiconductors. The real part of the dielectric constant relates to dispersion in the material, whereas the dissipative rate of the electromagnetic wave in the dielectric medium is provided by imaginary partand can be evaluated from the following equations [36]:

$$\varepsilon_i = 2nk \quad \text{and} \quad \varepsilon_r = n^2 - k^2 \tag{16}$$

The variation of ε_i and ε_r with λ for the as-prepared and annealed CdTe/CdSe bi-layer thin films is shown in **Fig. 8 (a- b),** respectively. The estimated values of $\varepsilon_r$and n for the tested thin films show a similar trend in the same spectrum of photon energy while the values of $\varepsilon_i$and k reveal similar behavior in the same range of photon energy. Also, values of ε_r were much greater than ε_i values. Although the imaginary part values ε_i enhanced with the increase in T_A in all the samples, the real part values showed a clear peak (absorption maxima) shifts towards lower energy as T_A increases.

Among the different quantities that are used to characterize the optical properties of thin films are is the dissipation factor, tan(δ), a measure of the loss of power in a mechanical phase, such as oscillation in the dissipative method- which may be computed as a function of ε_i and ε_r utilizing the following relation[37]:

$$\tan\delta = \frac{\varepsilon_i}{\varepsilon_r} \qquad (17)$$

The variations of dissipation factor as a function of photon energy were shown in **Fig. 9** This figure shows that the dissipation factor increases with increasing photon energyof the studied samples. On other hand, the positions of relaxation peaks were slightly shifted to lower energy as a result of increase of annealing temperature.

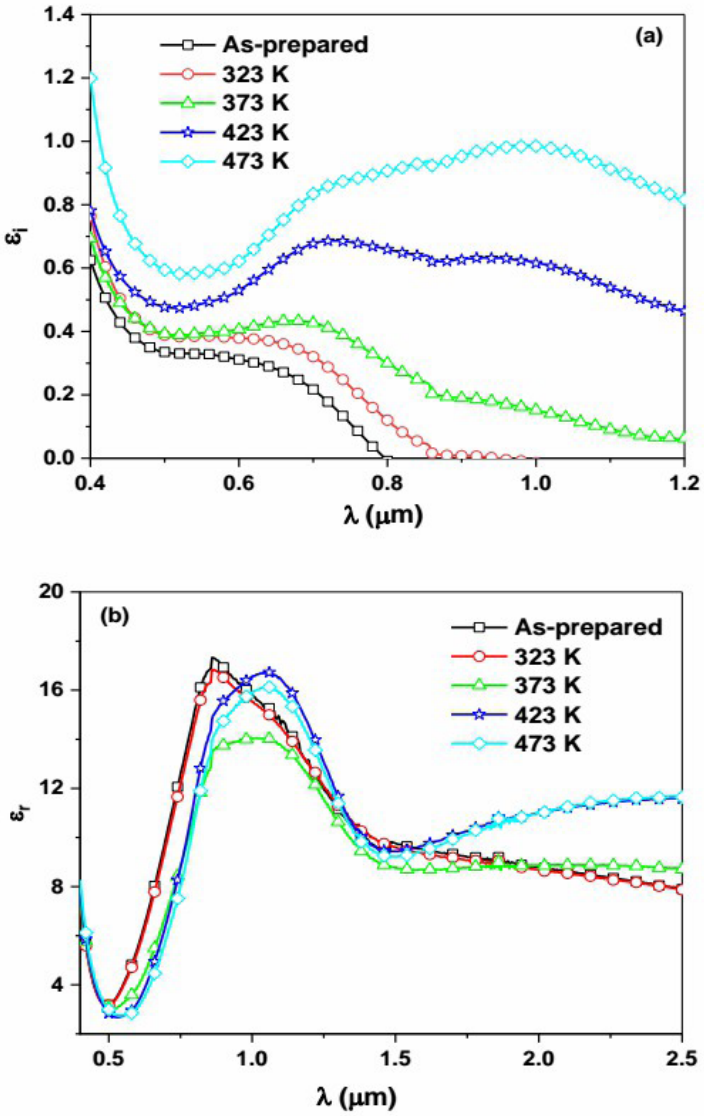

Fig. 8: Spectral distribution of, (a) the imaginary (ε_i) and (b) the real (ε_r) parts of the dielectric constant for CdTe/CdSe bi-layer thin films.

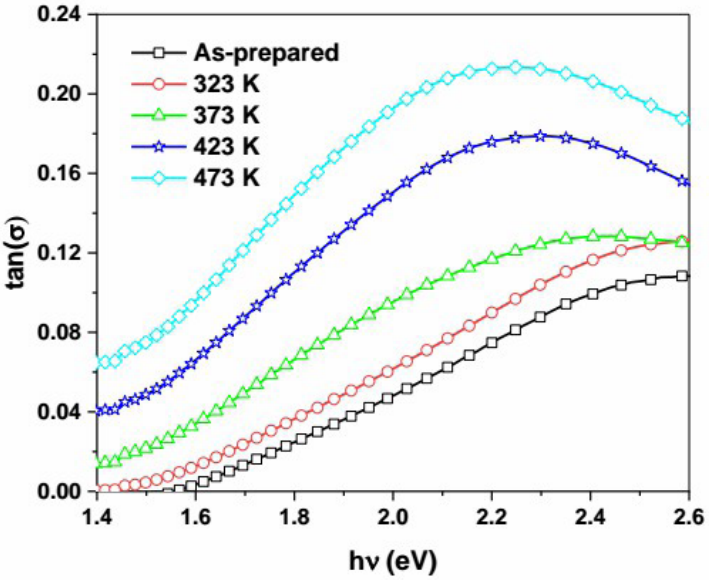

Fig. 9: Dependence of dissipation factor tan(δ) on the photon energy (hν)for CdTe/CdSe bi-layer thin films.

3.4 Optical conductivity

The optical conductivity $\sigma_{opt}$is an optical parameter that provides information about the electronic state in the material. Notably, the optical parameters α and *n* have been used to estimate the value of σ_{opt}as follows [38]:

$$\sigma_{opt.} = \frac{\alpha n c}{4\pi} \tag{18}$$

where *α*the absorption coefficient and *c* is the velocity of light. The variation in σ_{opt} against hν for as-prepared and annealed CdTe/CdSe bi-layer thin films is shown in **Fig. 10**. The deduced values of σ_{opt}

https://doi.org/10.54582/TSJ.2.2.52

reveal a linear behavior that directly proportional to both α and *n* based on **Eq. 18**.The increase of optical conductivity at high photon energies may be a result of the high absorbance of thin films and to the electron excited by photon energy [39]. It is obtained that the σ_{opt} values decreased with increasing T_A up to 373 K and then increased for annealing at T_A = 473 K.

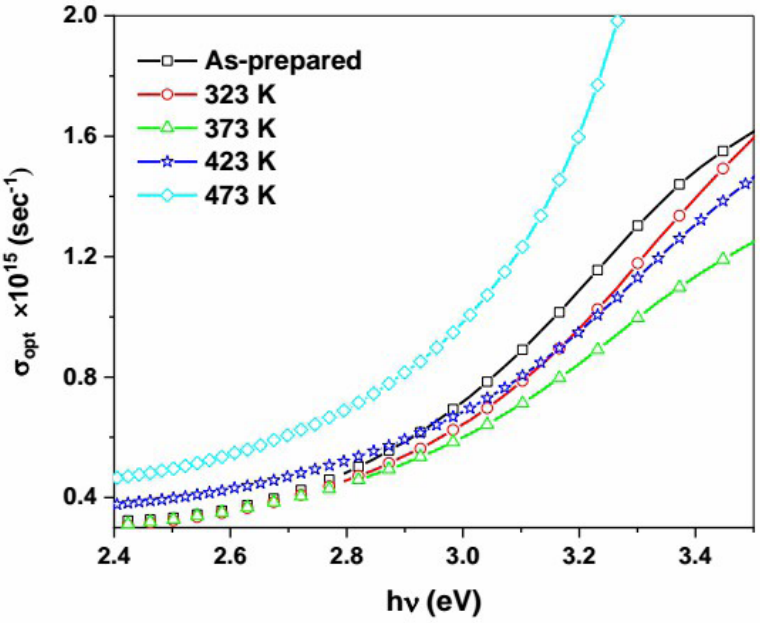

Fig. 10: Dependence of optical conductivity (σ_{opt}) on the photon energy (hν) for CdTe/CdSe bi-layer thin films.

3.5 The energy loss functions

Energy absorption by the material which might be due to single electron transitions or to collective effects induced within the solid can

be expressed in terms of the volume $(-I_m\ (1/\varepsilon))$ and surface $(-I_m\ (1/\varepsilon+1))$ energy loss functions which describe the probability that fast electrons will lose energy when traveling the bulk and surface of the material, respectively [40]. The energy-loss functions are related to real and imaginary parts, ε_r and ε_i, of the complex dielectric constant by the following relations [41]:

$$-I_m\left[\frac{1}{\varepsilon}\right]=\left[\frac{\varepsilon_i^2}{(\varepsilon_r^2+\varepsilon_i^2)}\right] \tag{19a}$$

$$-I_m\left[\frac{1}{\varepsilon+1}\right]=\left[\frac{\varepsilon_i^2}{(\varepsilon_r+1)^2+\varepsilon_i^2}\right] \tag{19b}$$

The dependency of both the volume (VELF) and surface (SELF) energy loss functions on photon energy in the fundamental absorption region for the investigated composition are shown in **Fig. 11(a-b)**, respectively. It is clear that the energy loss by the free charge carriers when traversing the bulk material has approximately the same value as when traversing the surface, in particular for relatively lower energies but the energy lost by the bulk volume of such films is greater than that lost by the surface at higher energies. With increase in T_A, the VELF and SELF values increase indicating the increased electron energy loss and the positions of relaxation peaks were slightly shifted to lower energy.

https://doi.org/10.54582/TSJ.2.2.52

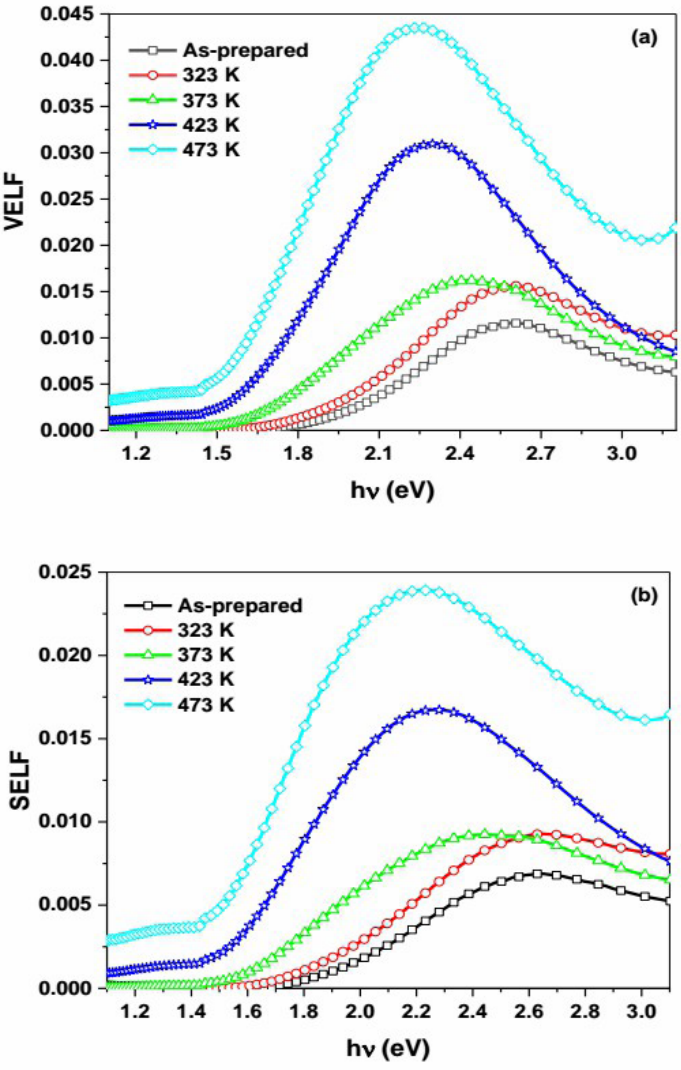

Fig. 11: The dependency of (a) VELF and (b) SELF functions on the photon energy for CdTe/CdSe bi-layer thin films.

https://doi.org/10.54582/TSJ.2.2.52

4. Conclusion

In summary, annealing-induced changes in the optical constants and dispersion parameters of thermally evaporated CdTe/CdSe bi-layer thin films were investigated in the UV–Vis-NIR wavelength region because of the absence of such information for these compositions in the literature. The most important findings are outlined as follows:

- The slight shift in transmission threshold towards higher wavelength region with increasing annealing temperature revealed the systematic reduction in optical energy band gap.
- The estimated value of k increased with an increase in annealing temperature, while the dispersion curve of the refractive index shows an anomalous dispersion in the absorption region and a normal dispersion in the transparent region.
- The maximum value of refractive index suffered a shift towards the longer wavelength as the annealing temperatures this behavior can be attributed to increase tailing.
- The dispersion of the refractive index studied utilizing the WDD single-oscillator model. The oscillator and dispersion parameters were computed as a function of annealing temperatures.
- The dispersion energy, E_d is increased with the incresese anneling temperatures, while the oscillator energy, E_o is decreased. The increase of E_d with the annealing temperature could be attributed

https://doi.org/10.54582/TSJ.2.2.52

to increasing the rate of atomic diffusion in the annealed thin films, indicating an increase in the number of atoms at interstitial sites which causes a formation of the impurity type scattering centers. The E_o, varied in proportion to optical band gap E_g, in accordance with the finding of Tanaka. The dispersion parameters: $N/m^*, \omega_p$, S_o and λ_o were found to be considerably sensitive to the annealing temperature of the investigated samples.

- In addition, we have discussed in details, the dielectric constants, optical conductivity and the energy loss functions. The increase in the optical conductivity value is good for the film to be used as the solar cell absorbing layer. The annealing temperature also significantly influences the VELF and SELF.A strong correlation between the evaluated data was also found and discussed well with the light of available reports.

References

1. El-Menyawy E. and A. Azab, "Optical, electrical and photoelectrical properties of nanocrystalline cadmium selenide films for photosensor applications", Optik, 2018.**168**: p. 217–227.

2. Mathuri S., K. Ramamurthi, and R.R. Babu," Influence of deposition distance and substrate temperature on the CdSe thin films

deposited by electron beam evaporation technique", Thin Solid Films, 2017. **625:** p. 138–147.

3. Taki M.," Structural and optical properties of Cadmium Telluride Cd_XTe_{1-X} thin film by evaporate technique", International Journal of Application or Innovation in Engineering & Management, 2013. **2(5):** p. 413–417.

4. Curtin, A.M., C.A. Vail, and H.L. Buckley, " CdTe in thin film photovoltaic cells: Interventions to protect drinking water in production and end-of-life", Water-Energy Nexus, 2020. **3:** p. 15-28.

5. Li, G., T. B. Chen, Z. Zhao, L. Ling, Q.Li, S. Chen, " Green and high yield synthesis of CdTe@Hydrotalcite nanocrystals with enhanced photoluminescence stability toward white light emitting diodes" J. Lumin., 2020. **228:** p. 117625.

6. Feng, H., J. Song, ,B. Song, Q. Lin, H. Shen, L.S Li, H. Wang, Z. Du, " Highly Efficient Near-Infrared Light-Emitting Diodes Based on Chloride Treated CdTe/CdSe Type-II Quantum Dots" Frontiers in chemistry, 2020. **8:** p. 266.

7. Harif, M.N., K.S.Rahman, H. N. Rosly, P. Chelvanathan, C. Doroody, H. Misran, N. Amin, " An approach to alternative post-deposition treatment in CdTe thin films for solar cell application" Superlattices Microstruct., 2020. **147**: p. 106687.

8. Himanshu, S.L Patel, A. Thakur, M. D. Kannan, M. S. Dhaka, "Impact of Bi doping on CdTe thin films: Thermal annealing

evolution of physical properties for solar cell absorber layer applications", 2020. **709:** p. 138004.

9. Maslyanchuk, O., M. Solovan, V. Brus, P. Maryanchuk, E. Maistruk, I. Fodchuk, V. Gnatyuk, "Charge transport features of CdTe-based X- and -ray detectors with Ti and TiO Schottky contacts", Nuclear Instruments and Methods in Physics Research Section A: Accelerators, Spectrometers, Detectors and Associated Equipment 2021. **988:** p. 164920.

10. Rizzo, A.,Y. Li, S. Kudera, F. Della Sala, M. Zanella, W. J. Parak, R. Cingolani, L. Manna, G. Gigli, "Blue light emitting diodes based on fluorescent CdSe/ZnS nanocrystals", Appl. Phys. Lett. **,** 2007. **90:** p. 051106.

11. Wu, B.J., L. H. Kuo, J. M. DePuydt, G. M. Haugen, M. A. Haase, L. Salamanca-Riba, "Growth and characterization of II–VI blue light-emitting diodes using short period superlattices", Appl. Phys. Lett.,. Phys. Lett. 1996. **68:** p.379-381.

12. Chander, S., and M.S. Dhaka, "Optimization of physical properties of vacuum evaporated CdTe thin films with the application of thermal treatment for solar cells", Mater. Sci. Semicond. Process., 2015. **40:** p. 708-712.

13. aIlican, S., Y. Caglara, M. Caglara, F.Yakuphanoglu, "The effects of substrate temperature on refractive index dispersion and optical

constants of $CdZn(S_{0.8}Se_{0.2})_2$ alloy thin films", J. Alloys Compd., 2009. **480**: p. 234–237.

14. Sun J., and J. Jasieniak," Semi-transparent solar cells", J. Phys. D Appl. Phys. 2017. **50**: p. 093001.

15. Dabban , M. A., and Abdel-naser A. Alfaqeer, "Enhancement in microstructural and optical properties of thermally evaporated CdTe/CdSe heterojunction thin films", University of Aden Journal and Applied Sciences, 2022. **26:2**: accepted for publication.

16. M. Murmann, "Die optischen Konstanten durchsichtigen Silbers", Z. Phys.1933. **80:** p. 161-177.

17. M. Murmann, "Der spektrale Verlauf der anomalen optischen Konstanten dünnen Silbers", Z. Phys. 1936. **101**: p. 643-648.

18. Abu El-Fadl, A. , M. M. Hafiz, M. M. Wakkad, A.S. Aashour, "Influence of γ-radiation on the optical parameters of $Ag_{10}Te_{90}$ thin films", Radiation Phy. & Chem., 2007. **76:** p. 61-66.

19. Abd-Elnaiem, A.M. , M. Mohamed, R.M. Hassan, M.A. Abdel-Rahim, A.A. Abu-Sehly, M.M. Hafiz, "Structural and optical characterization of annealed $As_{30}Te_{60}Ga_{10}$ thin films prepared by thermal evaporation technique". Mater. Sci. Pol.2018. **36:2:** P. 193–202.

20. Kumar, S., S. C. Kashyap, and K. L. Chopra, "Electron transport properties of n-type bismuth modified a-$Ge_{20}Se_{70}$ films", J. Non-Cryst. Solids, 1986. **85:** p. 100-104.

21. Wemple, S. H., and M. Didomenico, "Behavior of the electronic dielectric constant in covalent and ionic materials", Phys. Rev. B, 1971. 3: p. 1338.

22. Wemple, S. H.,"Refractive-index behavior of amorphous semiconductors and glasses", Phys. Rev. B, 1973. **7:** p. 3767.

23. Shaaban, E.R., M.Y. Hassaan, M.G. Moustafa, Ammar Qasem, Gomaa A.M. Ali, El Sayed Yousef, "Optical constants, dispersion parameters and non-linearity of different thickness of $As_{40}S_{45}Se_{15}$ thin films for optoelectronic applications", Optik, 2019. **186:** p. 275–287.

24. Tanaka, K., "Structural phase transitions in chalcogenide glasses, Phys. Rev. B, 1989. **39:** p. 1270.

25. Moss, T. S., "A relationship between the refractive index and the infrared threshold of sensitivity for photoconductors", Proc. Phys. Soc. B, 1950. **63:** p. 167.

26. Yakuphanoglu, F., A. Cukurovali, İ. Yilmaz, "Single-oscillator model and determination of optical constants of some optical thin film materials", Phys. B: Condens. Matter, 2004. **353**: p. 210–216.

27. Usha, K. S., R. Sivakumar, and C. Sanjeeviraja, "Optical constants and dispersion energy parameters of NiO thin films prepared by radio frequency magnetron sputtering technique", Journal of Applied Physics, 2013. **114**: p.123501.

28.Wemple, S. H., J. D. Gabbe, and G. D. Boyd, "Refractive index behavior of ternary chalcopyrite semiconductors", J. Appl. Phys. 1975. **46:** p. 3597.

29. Akl, A. A., "Thermal annealing effect on the crystallization and optical dispersion of sprayed V2O5 thin films", J. Phys. Chem. Solids 2010. **71**: p. 223.

30. Wolaton, A. K. , and T. S. Moss, "Determination of Refractive Index and Correction to Effective Electron Mass in PbTe and PbSe", Proc. Roy. Soc. (1963) **81:** p. 509-513.

31. Lee, P. A., G. Said, R. Davis, T. H. Lim, "On the optical properties of some layer compounds", J. Phys. Chem. Solids, 1969. **30:** p. 2719-2729.

32. Didomenico, M., and S. H. Wemple, "Oxygen-octahedra ferroelectrics. I. Theory of electro-optical and nonlinear optical effects", J. Appl. Phys., 1969. **40**: p. 720-734.

33. Zemel, J. N., J. D. Jensen, R. B. Schoolar, "Electrical and optical properties of epitaxial films of PbS, PbSe, PbTe, and SnTe", Phys. Rev. A, 1965. **140:** p. 330.

34. Yakuphanoglu, F., and C. Viswanathan, "Electrical conductivity and single oscillator model properties of amorphous CuSe semiconductor thin film", J. Non-Cryst. Solids, 2007. **353:** p. 2934-2937.

35. Penn, D. R., "Wave number-dependent dielectric function of semiconductors". Phys. Rev., 1962. **128:** p. 2093–2097.

36. El.-Korashy, A., H. El-Zahed, and M. Radwan, "Optical studies of [N(CH3)4]2CoCl4,[N(CH3)4]2MnCl4 single crystals in the normal paraelectric phase", Physica B, 2003. **334:** p. 75-81.

37. El-Nahass, M. M., A. M. Farag, K. F. Abdel-Rahman, A. A. Darwish, "Dispersion studies and electronic transitions in nickel phthalocyanine thin films" Opics & Laser Technology, 2005. **37(7)**: p. 513-523.

38. Kumar, V., and B. S. R. Sastry, "Heat of formation of ternary chalcopyrite semiconductors", J. Phys. Chem. Solids (2005. **66(1)**: p. 99–102.

39. Yakuphanoglu, F., A. Cukurovali, I. Yilmaz, "Refractive index and optical absorption properties of the complexes of a cyclobutane containing thiazolylhydrazone ligand", Opt. Mater., 2005. **27:** p. 1363 1368.

40. El-Nahass, M. M., H. S. Soliman, A. A. Hendi, and Sh. El-Gamdy, "Effect Of Annealing On The Structural And Optical Properties Of Tertracyanoquinodimethane Thin Films" Aust. J. Basic Appl. Sci. 2011. **5(6):** p. 145-156 (2011).

41. Pankove, J. I., "Optical processes in Semiconductors", Dover Publications Inc., New York, 1975.